SCIENTIFIC
REPORTS
natureresearch

OPEN

The Intrinsic Enzyme Activities of the Classic Polyoxometalates

Boyu Zhang, Mingming Zhao, Yanfei Qi*, Rui Tian, Boye B. Carter, Hangjin Zou, Chuhan Zhang & Chunyan Wang

The mimicking enzyme activities of eighteen classic POMs with different structures, Keggin ($H_3PW_{12}O_{40}$, $H_4SiW_{12}O_{40}$, $H_4GeW_{12}O_{40}$, $K_4GeW_{12}O_{40}$, $H_3PMo_{12}O_{40}$, $H_4SiMo_{12}O_{40}$ and $Eu_3PMo_{12}O_{40}$), Wells-Dawson ($H_6P_2Mo_{18}O_{62}$, α-$(NH_4)_6P_2W_{18}O_{62}$ and α-$K_6P_2W_{18}O_{62}\cdot 14H_2O$), lacunary-Keggin ($Na_8H[\alpha\text{-}PW_9O_{34}]$, $Na_{10}[\alpha\text{-}SiW_9O_{34}]$, $Na_{10}[\alpha\text{-}GeW_9O_{34}]$ and $K_8[\gamma\text{-}SiW_{10}O_{36}]$), the transition-metal substituted-type (α-1,2,3-$K_6H[SiW_9V_3O_{34}]$ and $H_5PMo_{10}V_2O_{40}$), sandwich-type ($K_{10}P_2W_{18}Fe_4(H_2O)_2O_{68}$) and an isopolyoxotungstate ($Na_{10}H_2W_{12}O_{42}$) were screened and compared. The mechanisms and reaction conditions of POMs with mimicking enzyme-like activities were also analyzed. The results shown that the structures, the hybrid atoms, the coordination atoms, the substituted metal atoms, pH and substrate are the effect factors for the enzyme mimic activities of POM. Among the eighteen POMs, $H_3PW_{12}O_{40}$, $H_4SiW_{12}O_{40}$, $H_4GeW_{12}O_{40}$, α-$(NH_4)_6P_2W_{18}O_{62}$, α-$K_6P_2W_{18}O_{62}\cdot 14H_2O$, $Na_8H[\alpha\text{-}PW_9O_{34}]$, $Na_{10}[\alpha\text{-}SiW_9O_{34}]$, $Na_{10}[\alpha\text{-}GeW_9O_{34}]$, $K_8[\gamma\text{-}SiW_{10}O_{36}]$, $K_{10}P_2W_{18}Fe_4(H_2O)_2O_{68}$ and $Na_{10}H_2W_{12}O_{42}$ had the peroxidase activities. $Eu_3PMo_{12}O_{40}$, $H_3PMo_{12}O_{40}$, $H_4SiMo_{12}O_{40}$, α-1,2,3-K_6H $[SiW_9V_3O_{34}]$, $H_6P_2Mo_{18}O_{62}$ and $H_5PMo_{10}V_2O_{40}$ showed the oxidase-like activities. $K_4GeW_{12}O_{40}$ did not show the peroxidase and oxidase activities. The $Na_8H[\alpha\text{-}PW_9O_{34}]$, $Na_{10}[\alpha\text{-}SiW_9O_{34}]$ and $Na_{10}[\alpha\text{-}GeW_9O_{34}]$ showed intrinsic enzyme activities at alkaline conditions, which were different from other type of POMs. The sandwich-type $K_{10}P_2W_{18}Fe_4(H_2O)_2O_{68}$ displayed the strongest peroxidase activity, which is similar to natural horseradish peroxidase.

Natural enzymes with high substrate specificity, activities and yields have attracted continuous scientific research interest. However, their intrinsic drawbacks, such as poor substrate versatility and assortment, low operational stabilities and low tolerance to environment conditions, limited their applications[1,2]. Therefore, artificial enzymes, as highly stable and low-cost alternatives to nature enzymes, attract continuing attention[3,4]. Constructing and screening highly efficient enzyme mimics is a tremendous motivator for researchers. To date, impressive development has been made in the field of artificial enzymes, and numerous diversity materials, such as supramolecular, porphyrins, nanoenzyme, and metal complexes have been extensively explored to mimic natural enzymes[5–9]. Generally, the efforts toward designing artificial enzymes with high activity can be divided in to two groups: the first is 'structural mimicking', which is to mimic the structure of enzymes, and the second is 'functional mimicking', which is to mimic enzymes that have similar activities[10]. Functional mimicking offers a straight forward method to discover new properties of functional materials, such as the discovery of nanoparticles with peroxidase-like activity, later referred to as nanozymes[9,11].

Polyoxometalates (POMs), a metal oxide cluster compounds, are combinations between oxygen and early transition metals at their high oxidation states[12,13]. The majority of the applications of POMs are found in the area of catalysis[14–16]. It is reported that POMs can catalyze H_2O_2-based epoxidation and oxidation of organic substrates by O_2 and H_2O_2 by multistep electron-transfer processes[17–19]. Therefore, it is not astonishing that POMs can used as enzyme mimics to catalyze H_2O_2-based oxidation of 3,3′,5,5′-tetramethylbenzidine (TMB) and Ortho-Phenylenediamine (OPD) to a colored complex which can be applied in bio- and chem-sensing, i.e., colorimetric detection of tumor cells and glucose. Wang *et al.* firstly found that folate-functionalized polyoxometalate nanoparticles have unique oxidase-like activity in colorimetric multiplexed immunoassay[20]. Moreover, they investigated the peroxidase mimetics of POMs ($H_3PW_{12}O_{40}$, $H_4SiW_{12}O_{40}$ and $H_3PMo_{12}O_{40}$) and $H_3PW_{12}O_{40}$/graphene in detection of glucose and H_2O_2[21]. Meanwhile, Sun *et al.* reported a simple, fast and sensitive colorimetric method to detect H_2O_2 based on $H_4SiW_{12}O_{40}$[19]. Furthermore, Wang *et al.* synthesized folate-functionalized POM hybrid nanoparticles ($FA\text{-}g\text{-}[(FeOH_2)_2SiW_{10}O_{36}]$ and $FA_nPMo_{12-n}V_nO_{40}$, $n = 1\text{–}3$) and studied the peroxidase-like activity in colorimetric assay of H_2O_2 and cancer cells[22]. These above early findings proved that the typical polyoxometalates and their hybrid nanoparticles have the enzyme mimics activities.

School of Public Health, Jilin University, Changchun, Jilin, 130021, China. *email: qiyanfei@jlu.edu.cn

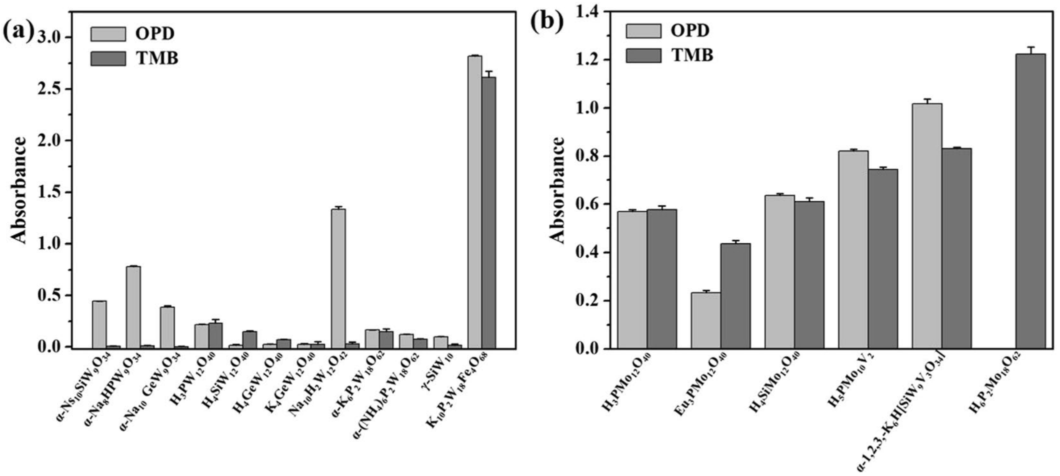

Figure 1. Comparison of enzyme mimic activities of polyoxometalates. (**a**) peroxidase-like activities with TMB or OPD as substrate. (**b**) oxidase-like activities with TMB or OPD as substrate. Conditions: 200 μM POMs, 200 mM H_2O_2 at room temperature for 10 minutes in the optimum pH.

POMs with different structural morphologies can incorporated with different metal atoms. The new inorganic compositions have presented attractive enzyme mimic features. For example, Li *et al.* synthesized three new tetra-nuclear Zr^{IV}- substituted POMs, which exhibit peroxidase-like activities[23]. Wang *et al.* established a colorimetric detection method based on the metal-substituted polyoxometalates of SiW_9M_3 ($M = Co^{2+}$, Fe^{3+}, Cu^{2+} and Mn^{2+})[24]. Xu *et al.* developed a Fe-containing heteropolyacid by cation-exchange and employed $KFePW_{12}O_{40}$ nanostructures for Fenton, photo-Fenton and enzyme-mimetic reactions[25].

POMs can assemble with functional materials to improve their properties and potential practical applications[26]. For instance, the dipeptide-POMs-graphene oxide ternary hybrid prepared by a precipitation method show a higher peroxidase activity compared to POMs alone[27]. Inorganic-organic hybrids based on POMs and transition-metal complexes are another similar strategy to construct new enzyme mimics. Gao *et al.* synthesized and structurally characterized two new hybrids based on copper(II)-imidazole complex modified sandwich-type tungstobismuthate or tungstoantimonite, $Na_4H_2[Cu_4(H_4im)_{12}(H_3im)_2][Cu_3(H_2O)_3(XW_9O_{33})_2] \cdot nH_2O$ (H_4im = imidazole, H_3im = deprotonated imidazole, X = Bi, Sb), which demonstrate higher peroxidase-like activity than Keggin-type POMs around physiological pH values in a heterogeneous phase[28]. Sha *et al.* isolated two new POM involved hybrids containing helix/nanocages ($[Cu^I_2Cu^{II}_2(fkz)_2(H_2O)_7(SiW_{12}O_{40})]$ and $[(Hfkz)_3(H_4SiW_{12}O_{40})]$) and systematically studied their peroxidase-like activities[29]. Rao *et al.* investigated the enzyme mimetic activity of a new inorganic-organic covalent hybrid of POM-calixarene[30]. Wei *et al.* reported the improved peroxidase-mimic property of the vesicles of hexavanadate-organic hybrid surfactants[31]. Metal-organic framework (MOF) based bio-sensing is a new interesting field. Pillar-layered MOFs have been proven to be an effective route to construct enzyme mimics with high stability and multifunction. The advancement of MOF structure is also help in design of new enzymes with POMs moiety. For example, Qin *et al.* report a novel efficient peroxidase mimic POM-pillared MOF, $Cu_6(Trz)_{10}(H_2O)_4[H_2SiW_{12}O_{40}] \cdot 8H_2O$[32]. Recently, *Sha et al.* reported a stable peroxidase mimic POM-pillared metal–MOF with 6-nuclear Cu-pz and 10-nuclear Cu-pz-Cl cycles, $[Cu_5(pz)_6Cl]\ [SiW_{12}O_{40}]$[33].

Most of the POMs are stable and show higher enzyme activities at acid condition (about pH value 3 or 4). However, in the physiological solutions (pH 7.0–7.5), for most bioanalytical applications, the POM nanozymes become catalytically inactive. Fortunately, POMs show a great diversity in its structure derived from its multiple oxidation states and coordination geometries[30,34]. These features make it much easier to control the size, shape, and charge distribution at the molecular level. Flexibility in the structure makes it possible to fine-tune the redox potentials, acidities, and enzyme activities of POMs. For example, the trivacant Keggin $Na_{10}[\alpha\text{-}SiW_9O_{34}]$ exhibits unusual peroxidase-like activity at basic condition[35]. Therefore, it is necessary to systematic investigate of POMs mimic enzymes activity with different structure category. Herein, the mimicking enzyme activities of classic polyoxometalates with different classic structures and different element atoms were screened and compared.

Results and Discussion

Characterization of POMs. The POMs were prepared according to the literature and identified by FI-IR spectra, UV-Vis spectra, as shown in Supplementary Figs S1 and S2.

Enzyme mimetic activities of POMs. As shown in Fig. 1, the enzyme mimetic activities of 18 POMs with Keggin structures ($H_3PW_{12}O_{40}$, $H_4SiW_{12}O_{40}$, $H_4GeW_{12}O_{40}$, $K_4GeW_{12}O_{40}$, $H_3PMo_{12}O_{40}$, $H_4SiMo_{12}O_{40}$ and $Eu_3PMo_{12}O_{40}$), Dawson structures ($H_6P_2Mo_{18}O_{62}$, $\alpha\text{-}(NH_4)_6P_2W_{18}O_{62}$ and $\alpha\text{-}K_6P_2W_{18}O_{62} \cdot 14H_2O$), lacunary-Keggin structures ($Na_8H[\alpha\text{-}PW_9O_{34}]$, $Na_{10}[\alpha\text{-}SiW_9O_{34}]$, $Na_{10}[\alpha\text{-}GeW_9O_{34}]$ and $K_8[\gamma\text{-}SiW_{10}O_{36}]$), the transition-metal substituted-type structures (α-1,2,3-$K_6H[SiW_9V_3O_{34}]$, $H_5PMo_{10}V_2O_{40}$) and sandwich-type $K_{10}P_2W_{18}Fe_4(H_2O)_2O_{68}$) were studied and compared at the same concentration with OPD and TMB as substrates. It was found that the coordination atoms, Mo and W, have effect on the enzyme mimic activity. All the polyoxotungstates $H_3PW_{12}O_{40}$, $H_4SiW_{12}O_{40}$, $H_4GeW_{12}O_{40}$, $K_4GeW_{12}O_{40}$, $Na_{10}[\alpha\text{-}GeW_9O_{34}]$, $Na_8H[\alpha\text{-}PW_9O_{34}]$, $Na_{10}[\alpha\text{-}SiW_9O_{34}]$, $K_8[\gamma\text{-}SiW_{10}O_{36}]$, $\alpha\text{-}(NH_4)_6P_2W_{18}O_{62}$, $\alpha\text{-}K_6P_2W_{18}O_{62}\cdot 14H_2O$, $Na_{10}H_2W_{12}O_{42}$ and $K_{10}P_2W_{18}Fe_4(H_2O)_2O_{68}$ are capable of catalyzing typical peroxidase reactions using both chromogenic heme-peroxidase substrates TMB and OPD in the presence of H_2O_2 to produce a blue color (maximum absorbance 650 nm) and brown color (maximum absorbance 450 nm) reaction, respectively, as shown in Fig. 1a. Initially, these reactions were carried out by adding 200 μM of POMs with the substrates OPD (576 μM) and H_2O_2 (200 mM) at room temperature in a buffered solution. It indicates that these POMs have intrinsic peroxidase-like activities towards these substrates (Fig. 1). However, the peroxidase-like activities of these POMs are different in the present of different substrates at the same concentration. For TMB as organic substrate, the absorption values of TMB^+ indicated that the order of peroxidase-like activities from high to low was $K_{10}P_2W_{18}Fe_4(H_2O)_2O_{68} > H_3PW_{12}O_{40} > H_4SiW_{12}O_{40} > \alpha\text{-}K_6P_2W_{18}O_{62}\cdot 14H_2O > \alpha\text{-}(NH_4)_6P_2W_{18}O_{62} > H_4GeW_{12}O_{40} > Na_{10}H_2W_{12}O_{42} > K_4GeW_{12}O_{40} > K_8[\gamma\text{-}SiW_{10}O_{36}] > Na_8H[\alpha\text{-}PW_9O_{34}] \approx Na_{10}[\alpha\text{-}SiW_9O_{34}] \approx Na_{10}[\alpha\text{-}GeW_9O_{34}]$. For OPD as organic substrate, the order of peroxidase-like activities from high to low was $K_{10}P_2W_{18}Fe_4(H_2O)_2O_{68} > Na_{10}H_2W_{12}O_{42} > Na_8H[\alpha\text{-}PW_9O_{34}] > Na_{10}[\alpha\text{-}SiW_9O_{34}] > Na_{10}[\alpha\text{-}GeW_9O_{34}] > H_3PW_{12}O_{40} > \alpha\text{-}K_6P_2W_{18}O_{62}\cdot 14H_2O > \alpha\text{-}(NH_4)_6P_2W_{18}O_{62} > K_8[\gamma\text{-}SiW_{10}O_{36}] > H_4GeW_{12}O_{40} \approx K_4GeW_{12}O_{40} \approx H_4SiW_{12}O_{40}$. From the results, the lacunary-Keggin POMs, $Na_{10}[\alpha\text{-}GeW_9O_{34}]$, $Na_8H[\alpha\text{-}PW_9O_{34}]$, $Na_{10}[\alpha\text{-}SiW_9O_{34}]$ and $Na_{10}H_2W_{12}O_{42}$ are higher affinity to the substrate of OPD than TMB. There are tiny absorbance peaks (OD values of 0.0100, 0.0070, 0.0017 and 0.0317) can be found in the above four POMs with TMB as substrates. The result indicated that peroxidase-like activities of POMs may substrate-dependence. However, no matter which the substrate was, the sandwich-type $K_{10}P_2W_{18}Fe_4(H_2O)_2O_{68}$ showed the highest peroxidase activity. Under the same substrate, it was found that the hybrid atoms had effect on the peroxidase activities of the POMs and the order was P > Si > Ge. In the same hybrid atom and TMB substrate, the peroxidase activity order is Keggin structure > Wells-Dawson > lacunary-Keggin. The reactions were also carried out in the absence of the POMs at their various suitable pH values, respectively. No significant unspecific oxidation reactions were observed [Supplementary Figs S3, S4] even after half an hour. Additional control experiments using POMs in absence of H_2O_2 showed that no oxidative reaction occurs. Hence, these POMs had only the peroxidase-like activities defeating many mimic enzyme peroxidases which also display oxidase-like activities. The enzymatic properties of these POMs are specificity and rarely reported in the literatures[11].

The polyoxomolybdates ($H_3PMo_{12}O_{40}$, $H_4SiMo_{12}O_{40}$, $Eu_3PMo_{12}O_{40}$, α-1,2,3,-$K_6H[SiW_9V_3O_{34}]$, $H_5PMo_{10}V_2O_{40}$ and $H_6P_2Mo_{18}O_{62}$) are capable of catalyzing oxidase reactions with both substrates TMB and OPD in the absence of H_2O_2 to produce a blue color (maximum absorbance 650 nm) and orange color (maximum absorbance 450 nm) reaction, respectively, as shown in Fig. 1b. Furthermore, the oxidase-like activities of these POMs are similar in the present of different substrates. For TMB as organic substrate, the absorption values indicated that the order of oxidase-like activities from high to low was $H_6P_2Mo_{18}O_{62} > \alpha\text{-}1,2,3\text{-}K_6H[SiW_9V_3O_{34}] > H_5PMo_{10}V_2O_{40} > H_4SiMo_{12}O_{40} > H_3PMo_{12}O_{40} > Eu_3PMo_{12}O_{40}$. For OPD as substrate, the order of oxidase-like activities from high to low was $\alpha\text{-}1,2,3\text{-}K_6H[SiW_9V_3O_{34}] > H_5PMo_{10}V_2O_{40} > H_4SiMo_{12}O_{40} > H_3PMo_{12}O_{40} > Eu_3PMo_{12}O_{40}$. In the OPD substrate, the color of $H_6P_2Mo_{18}O_{62}$ catalytic reaction solution became dark blue with a maximum absorption peak at 710 nm. The maximum absorption peak matched with the hybrid blue, the reduction product of $H_6P_2Mo_{18}O_{62}$, which covered the absorption peak of the oxide product of OPD. Therefore, only TMB was chosen as the substrate for $H_6P_2Mo_{18}O_{62}$. Finally, $K_4GeW_{12}O_{40}$ did not show the peroxidase and oxidase activities.

Effect of pH. The effect of pH on the catalytic activities of different types of POMs was measured by varying the pH and keeping the OPD and H_2O_2 concentration constant. The absorbance value of DAB with $H_3PW_{12}O_{40}$ and $Na_{10}H_2W_{12}O_{42}$ reached a maximum at the pH 2.5, as shown in Fig. 2a,b. After exceeding this point, the absorbance decreased gradually as increasing pH values. Therefore, pH 2.5 was selected as the optimal pH value for $H_3PW_{12}O_{40}$ and $Na_{10}H_2W_{12}O_{42}$. Similarly, pH 5 was selected as the optimal pH value for $K_{10}P_2W_{18}Fe_4(H_2O)_2O_{68}$, as shown in Fig. 2c. Interestingly, the catalytic activity of the $Na_{10}[\alpha\text{-}GeW_9O_{34}]$, $Na_8H[\alpha\text{-}PW_9O_{34}]$ and $Na_{10}[\alpha\text{-}SiW_9O_{34}]$ shows a pH optimum at alkaline conditions (~10). At this pH and in the absence of $Na_{10}[\alpha\text{-}GeW_9O_{34}]$, $Na_8H[\alpha\text{-}PW_9O_{34}]$ and $Na_{10}[\alpha\text{-}SiW_9O_{34}]$ the unspecific reaction between OPD (576 μM) and H_2O_2 (200 mM) was not observed. As mentioned, most of the known peroxidase-like POMs based artificial enzymes show their high activities at acid condition. Some POMs hybrids, such as inorganic-organic hybrids and FA functional particles exhibit oxidation catalyst at pH about 7.0[22,25]. However, $Na_{10}[\alpha\text{-}GeW_9O_{34}]$, $Na_8H[\alpha\text{-}PW_9O_{34}]$ and $Na_{10}[\alpha\text{-}SiW_9O_{34}]$ are highly active even at pH above 10, as shown in Fig. 2d–f. Based on the catalytic properties of these trivacant Keggin heterotungstates, we build a CdTe quantum dots (QDs)-based fluorometric method for sensitive detection of hydrogen peroxide[35]. The effect of pH on the catalytic activities of $H_3PW_{12}O_{40}$ and $K_{10}P_2W_{18}Fe_4(H_2O)_2O_{68}$ with TMB as substrate were also investigated, as shown in Supplementary Fig. S5. The optimal pH for $H_3PW_{12}O_{40}$ and $K_{10}P_2W_{18}Fe_4(H_2O)_2O_{68}$ were 2.5 and 4, respectively.

Analogously, the reaction pH-dependent response curves on oxidase mimics $H_3PMo_{12}O_{40}$, $H_4SiMo_{12}O_{40}$, $Eu_3PMo_{12}O_{40}$, $H_5PMo_{10}V_2O_{40}$ and $\alpha\text{-}1,2,3\text{-}K_6H\text{-}[SiW_9V_3O_{34}]$ with OPD as substrates and $H_6P_2Mo_{18}O_{62}$ with TMB as substrate were shown in Fig. 3. When the pH value increased from 2.0 to 7, the absorbance reached the maximums at pH 4, 5, 3, 2.5, 4 and 5 for $H_3PMo_{12}O_{40}$, $H_4SiMo_{12}O_{40}$, $Eu_3PMo_{12}O_{40}$, $H_5PMo_{10}V_2O_{40}$, $\alpha\text{-}1,2,3\text{-}K_6H[SiW_9V_3O_{34}]$ and $H_6P_2Mo_{18}O_{62}$, respectively. The effect of pH on the catalytic activities of $H_3PMo_{12}O_{40}$, $H_4SiMo_{12}O_{40}$, $Eu_3PMo_{12}O_{40}$, $H_5PMo_{10}V_2O_{40}$ and $\alpha\text{-}1,2,3\text{-}K_6H[SiW_9V_3O_{34}]$ with TMB as substrate were also investigated, as shown in Supplementary Fig. S6. When TMB as substrates, $H_3PMo_{12}O_{40}$, $H_4SiMo_{12}O_{40}$, $Eu_3PMo_{12}O_{40}$, $H_5PMo_{10}V_2O_{40}$ and $\alpha\text{-}1,2,3\text{-}K_6H[SiW_9V_3O_{34}]$ exhibited their strongest activities when the pH was 4, 5, 4, 2.5 and 4, respectively.

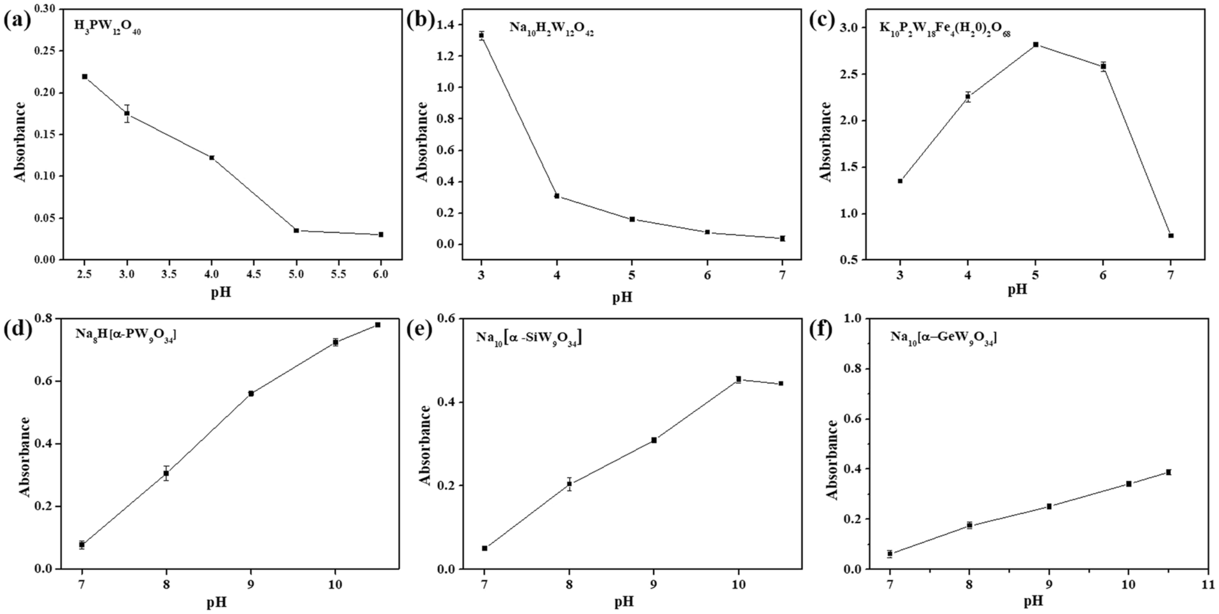

Figure 2. Effects of pH on peroxidase-like enzymes with OPD as a substrate, respectively. (**a**) $H_3PW_{12}O_{40}$; (**b**) $Na_{10}H_2W_{12}O_{42}$; (**c**) $K_{10}P_2W_{18}Fe_4(H_2O)_2O_{68}$; (**d**) $Na_8H[\alpha\text{-}PW_9O_{34}]$; (**e**) $Na_{10}[\alpha\text{-}SiW_9O_{34}]$; (**f**) $Na_{10}[\alpha\text{-}GeW_9O_{34}]$; Conditions: 200 μM POMs, 200 mM H_2O_2, 0.2 mM Na_2HPO_4-citrate buffer for $H_3PW_{12}O_{40}$, $Na_{10}H_2W_{12}O_{42}$ and $K_{10}P_2W_{18}Fe_4(H_2O)_2O_{68}$; 0.1 mM Tris-HCl for $Na_8H[\alpha\text{-}PW_9O_{34}]$, $Na_{10}[\alpha\text{-}SiW_9O_{34}]$ and $Na_{10}[\alpha\text{-}GeW_9O_{34}]$ at room temperature for 10 minutes. The error bars represent the standard deviation of three measurements.

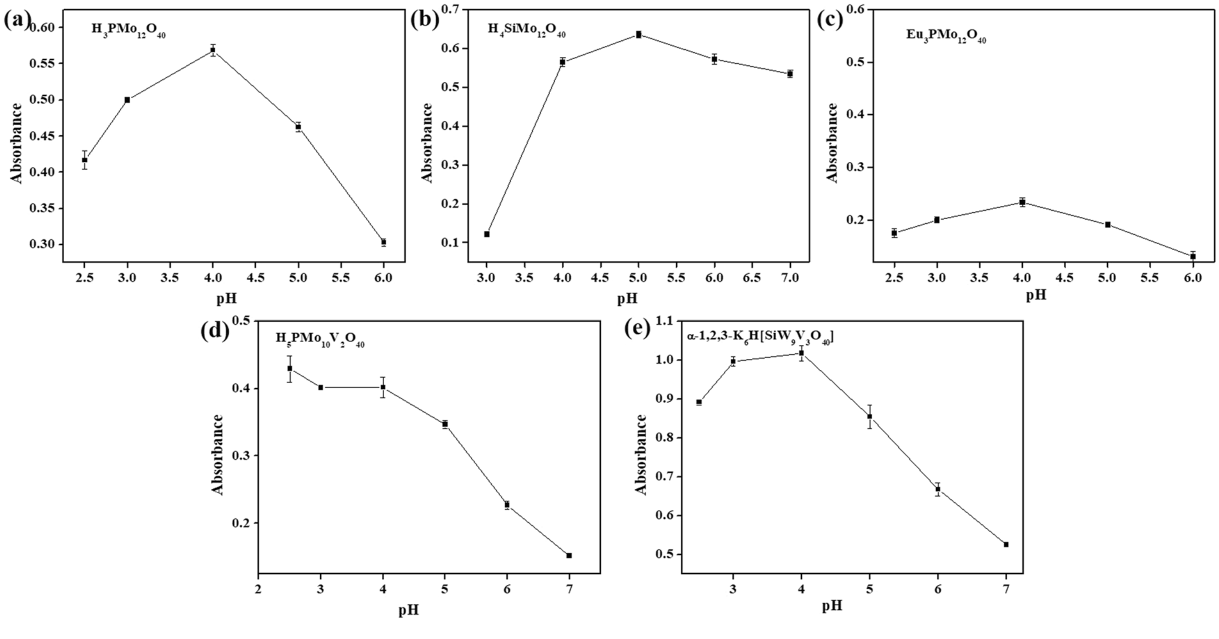

Figure 3. Effects of pH on oxidase-like enzymes with OPD as a substrate. (**a**) $H_3PMo_{12}O_{40}$; (**b**) $H_4SiMo_{12}O_{40}$; (**c**) $Eu_3PMo_{12}O_{40}$; (**d**) $H_5PMo_{10}V_2O_{40}$; (**e**) $\alpha\text{-}1,2,3\text{-}K_6H[SiW_9V_3O_{34}]$; (**f**) $H_6P_2Mo_{18}O_{62}$ with TMB as substrates. Conditions: 200 μM POMs, 200 mM H_2O_2, 0.2 mM Na_2HPO_4-citrate buffer at room temperature for 10 minutes. The error bars represent the standard deviation of three measurements.

Effect of concentration of POMs. The OPD oxidation rate catalyzed by the peroxidase-like POMs was dependent on the concentration of these POMs with the other parameters were kept constant, as shown in Fig. 4. In a typical experiment, the POMs oxidation activity was determined by monitoring of the absorbance at 450 nm (which increases because of DAB, the oxidation product of OPD, formation) for 10 min at 25 °C in different buffer for varying concentrations of POMs with respect to OPD (576 μM) and H_2O_2 (200 mM). It can be found that the greater the amount of catalyst, the higher the yield of DAB. The increasing of the DAB yield becomes gentle when the amount of $H_3PW_{12}O_{40}$, $Na_{10}H_2W_{12}O_{42}$, $Na_{10}[\alpha\text{-}GeW_9O_{34}]$, $Na_8H[\alpha\text{-}PW_9O_{34}]$,

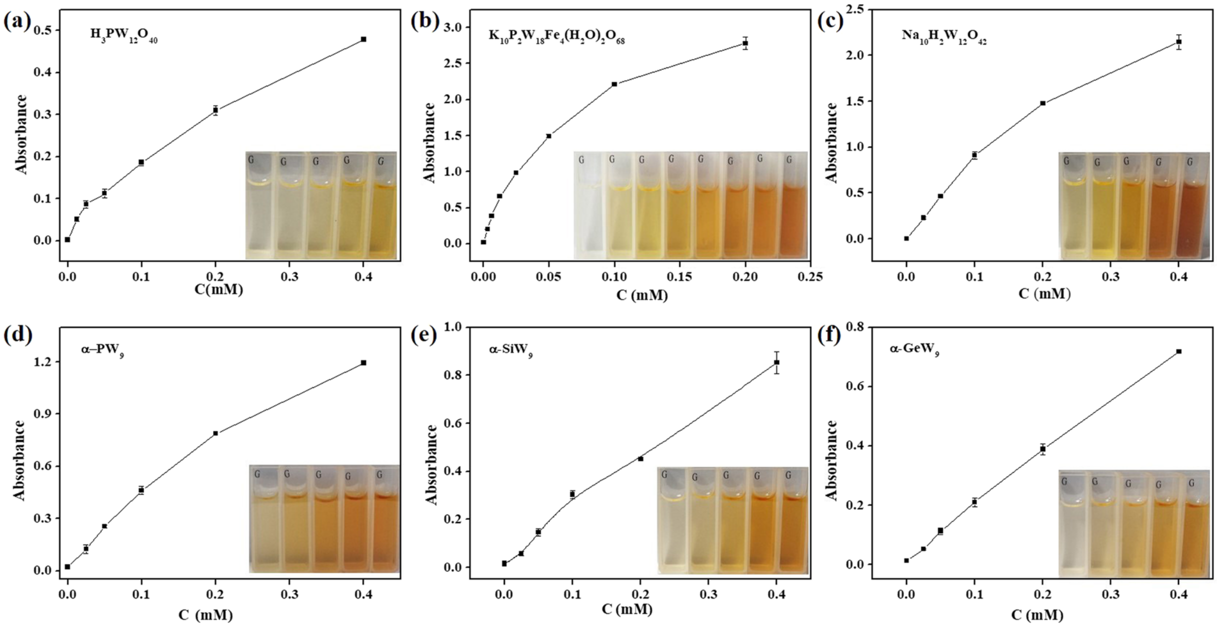

Figure 4. Effects of concentrations of peroxidase-like enzymes with OPD as a substrate. (**a**) $H_3PW_{12}O_{40}$; (**b**) $Na_{10}H_2W_{12}O_{42}$; (**c**) $K_{10}P_2W_{18}Fe_4(H_2O)_2O_{68}$; (**d**) Na_8H[α-PW_9O_{34}]; (**e**) Na_{10}[α-SiW_9O_{34}]; (**f**)Na_{10}[α-GeW_9O_{34}]; Conditions: 200 mM H_2O_2, 0.2 mM Na_2HPO_4-citrate buffer for $H_3PW_{12}O_{40}$, $Na_{10}H_2W_{12}O_{42}$ and $K_{10}P_2W_{18}Fe_4(H_2O)_2O_{68}$; 0.1 mM Tris-HCl for Na_8H[α-PW_9O_{34}], Na_{10}[α-SiW_9O_{34}] and Na_{10}[α-GeW_9O_{34}] at room temperature for 10 minutes. The error bars represent the standard deviation of three measurements.

Na_{10}[α-SiW_9O_{34}] and $K_{10}P_2W_{18}Fe_4(H_2O)_2O_{68}$ exceeds 0.4, 0.4, 0.4, 0.4, 0.4 and 0.1 mM, respectively. Furthermore, Na_{10}[α-GeW_9O_{34}], Na_8H[α-PW_9O_{34}] and Na_{10}[α-SiW_9O_{34}] were insoluble when the concentrations were beyond 0.4 mM. Therefore, 0.4 mM was chosen as the optimum concentrations of $H_3PW_{12}O_{40}$, $Na_{10}H_2W_{12}O_{42}$, Na_{10}[α-GeW_9O_{34}], Na_8H[α-PW_9O_{34}] and Na_{10}[α-SiW_9O_{34}] for the kinetics experiments. While, 0.1 mM was chosen for $K_{10}P_2W_{18}Fe_4(H_2O)_2O_{68}$. The effect of the amounts of $H_3PW_{12}O_{40}$ and $K_{10}P_2W_{18}Fe_4(H_2O)_2O_{68}$ on peroxidase-like activities with TMB as substrates were also investigated, as shown in Supplementary Fig. S7. 0.4 mM and 0.1 mM were chosen for $H_3PW_{12}O_{40}$ and $K_{10}P_2W_{18}Fe_4(H_2O)_2O_{68}$ as the optimum concentrations, respectively.

As shown in Fig. 5, the effect of the amounts of POMs with oxidase-like activities on the yield of DAB was also investigated. The procedures were similar with above except H_2O_2. DAB is obtained without H_2O_2, while the absorbance of DAB increases along with the increase in the amount of $H_3PMo_{12}O_{40}$, $H_4SiMo_{12}O_{40}$ and $Eu_3PMo_{12}O_{40}$ and reached the maximum at 0.4 mM POMs. The maximum concentrations of $H_5PMo_{10}V_2$ and α-1,2,3-$K_6H[SiW_9V_3O_{34}]$ were 0.2 mM. The maximum concentration of $H_6P_2Mo_{18}O_{62}$ with TMB as substrates was 50 μM. As shown in Fig. S8, when TMB were substrates, we found that the optimum concentration was 0.1 mM for $H_3PMo_{12}O_{40}$, $H_5PMo_{10}V_2$ and α-1,2,3- $K_6H[SiW_9V_3O_{34}]$. $H_4SiMo_{12}O_{40}$ and $Eu_3PMo_{12}O_{40}$ reached their maximum absorption values when the concentrations were 0.2 mM and 0.4 mM, respectively.

Effect of reaction time. The variation of the DAB yield with increasing reaction time is shown in Fig. 6. It can be observed that absorption value of DAB reaches a maximum during a reaction time of less than 10 minutes and 1 minute for peroxidase and oxidase when 200 mM H_2O_2 and 576 μM OPD were used, respectively. After that, along with the increasing of reaction time, the yield of DAB remains nearly constant. This indicates that the optimized reaction time were 10 minutes for $H_3PW_{12}O_{40}$, Na_{10}[α-GeW_9O_{34}], Na_8H[α-PW_9O_{34}] and Na_{10}[α-SiW_9O_{34}], 5 minutes for $K_{10}P_2W_{18}Fe_4(H_2O)_2O_{68}$ and 2 minutes for $Na_{10}H_2W_{12}O_{42}$, as shown in Fig. 6a. The reaction time for oxidase were less than 60 s for $H_3PMo_{12}O_{40}$, $H_4SiMo_{12}O_{40}$, $Eu_3PMo_{12}O_{40}$, $H_5PMo_{10}V_2O_{40}$, α-1,2,3-$K_6H[SiW_9V_3O_{34}]$ and $H_6P_2Mo_{18}O_{62}$.

Kinetic parameters. The mechanism of peroxidase-like catalytic activities of $K_{10}P_2W_{18}Fe_4(H_2O)_2O_{68}$, $H_3PW_{12}O_{40}$, $H_4SiW_{12}O_{40}$, Na_{10}[α-GeW_9O_{34}], Na_8H[α-PW_9O_{34}], Na_{10}[α-SiW_9O_{34}] and $Na_{10}H_2W_{12}O_{42}$ was further investigated using steady-state kinetics. It has been observed that OPD oxidation catalysis mediated by these POMs is dependent on the substrate concentration. In order to study activities of POMs, several experiments were performed whereby the concentration of either OPD or H_2O_2 was varied while keeping the other concentration constant. The concentration of the POMs was kept constant in all these experiments. The oxidation reaction catalyzed by $K_{10}P_2W_{18}Fe_4(H_2O)_2O_{68}$, $H_3PW_{12}O_{40}$, $H_4SiW_{12}O_{40}$, Na_{10}[α-GeW_9O_{34}], Na_8H[α-PW_9O_{34}], Na_{10}[α-SiW_9O_{34}] and $Na_{10}H_2W_{12}O_{42}$ follows a Michaelis-Menten behavior. The K_m and V_{max} of $K_{10}P_2W_{18}Fe_4(H_2O)_2O_{68}$ and $H_3PW_{12}O_{40}$ were obtained using a Line weaver-Burk plot with OPD as substrates, as shown in Fig. 7. The K_m and V_{max} of $K_{10}P_2W_{18}Fe_4(H_2O)_2O_{68}$ with H_2O_2 as substrates were 0.113 mM and 1.13×10^{-9} M·S^{-1} in OPD system, as shown in Fig. 7a. The K_m and V_{max} of $K_{10}P_2W_{18}Fe_4(H_2O)_2O_{68}$ with OPD as substrates were 0.109 mM and 4.11×10^{-8} M·S^{-1},

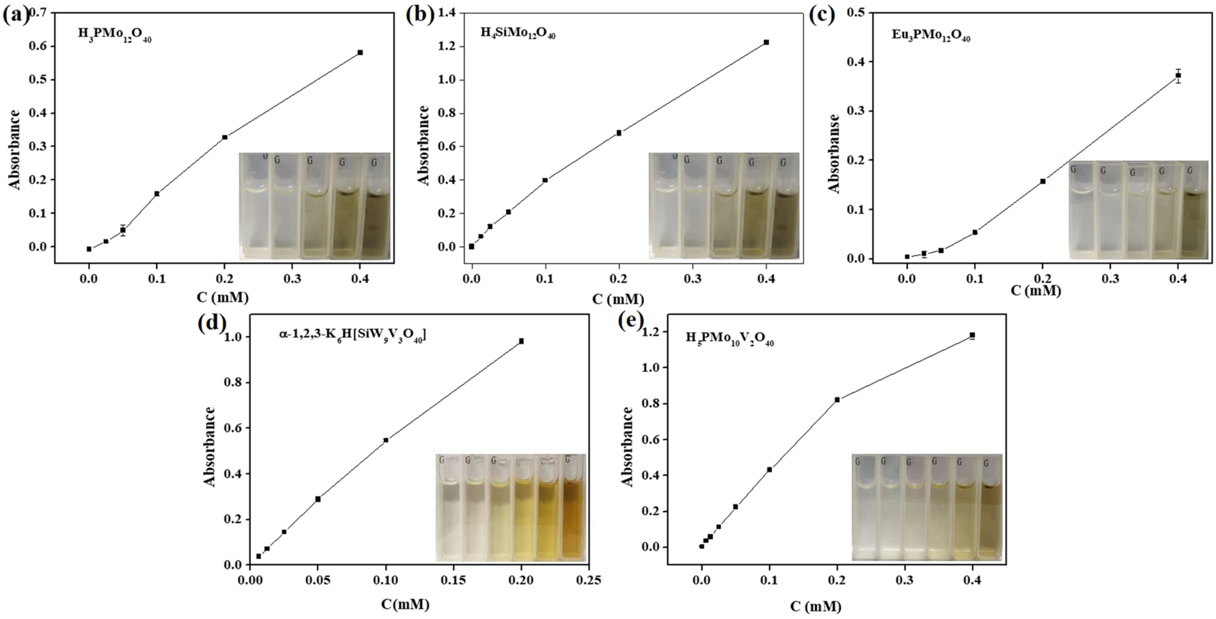

Figure 5. Effects of concentrations of oxidase-like enzymes with OPD as a substrate. (**a**) $H_3PMo_{12}O_{40}$; (**b**) $H_4SiMo_{12}O_{40}$; (**c**)$Eu_3PMo_{12}O_{40}$; (**d**)$H_5PMo_{10}V_2O_{40}$; (**e**)α-1,2,3-$K_6H[SiW_9V_3O_{34}]$; (**f**)$H_6P_2Mo_{18}O_{62}$ with TMB as substrates. Conditions: 0.2 mM Na_2HPO_4-citrate buffer at room temperature for 10 minutes.The error bars represent the standard deviation of three measurements.

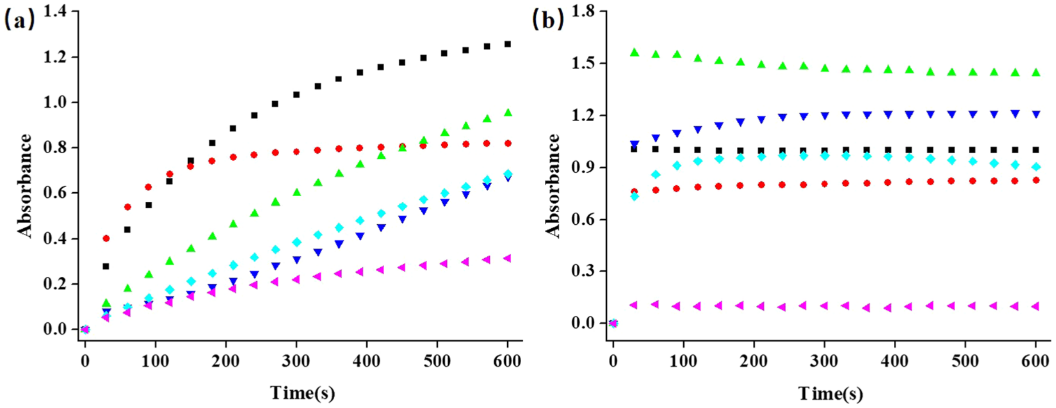

Figure 6. The reaction time of different-type POMs. (**a**) peroxidase (black: $K_{10}P_2W_{18}Fe_4(H_2O)_2O_{68}$; red: $Na_{10}H_2W_{12}O_{42}$; green: $Na_8H[\alpha\text{-}PW_9O_{34}]$; light blue: $[\alpha\text{-}SiW_9O_{34}]$; dark blue: $Na_{10}[\alpha\text{-}GeW_9O_{34}]$; pink: $H_3PW_{12}O_{40}$); (**b**) oxidase (green: $H_6P_2Mo_{18}O_{62}$; dark blue: α-1,2,3-$K_6H[SiW_9V_3O_{34}]$; black: $H_5PMo_{10}V_2O_{40}$; light blue: $H_4SiMo_{12}O_{40}$; red: $H_3PMo_{12}O_{40}$; pink: $Eu_3PMo_{12}O_{40}$).

as shown in Fig. 7b. The K_{cat} of $K_{10}P_2W_{18}Fe_4(H_2O)_2O_{68}$ with H_2O_2 and OPD are $3.22 \times 10^{-3}\,S^{-1}$ and $3.80 \times 10^{-3}\,S^{-1}$. The K_m and V_{max} of $H_3PW_{12}O_{40}$ with H_2O_2 as substrates were 6.624 mM and 3.89×10^{-9} M·S^{-1} in OPD system, as shown in Fig. 7c. The K_m and V_{max} of $H_3PW_{12}O_{40}$ with OPD as substrates were 0.174 mM and 6.14×10^{-9} M·S^{-1}, as shown in Fig. 7d. The K_{cat} of $H_3PW_{12}O_{40}$ with H_2O_2 and OPD are $8.22 \times 10^{-4}\,S^{-1}$ and $2.83 \times 10^{-6}\,S^{-1}$. As shown in Fig. 8, the values for K_m OPD of $Na_8H[\alpha\text{-}PW_9O_{34}]$, $Na_{10}[\alpha\text{-}SiW_9O_{34}]$, $Na_{10}[\alpha\text{-}GeW_9O_{34}]$ and $Na_{10}H_2W_{12}O_{42}$ were 1.39, 0.854, 0.611 and 0.205 mM, respectively. The values for V_{max} OPD of $Na_8H[\alpha\text{-}PW_9O_{34}]$, $Na_{10}[\alpha\text{-}SiW_9O_{34}]$, $Na_{10}[\alpha\text{-}GeW_9O_{34}]$ and $Na_{10}H_2W_{12}O_{42}$ were 2.53×10^{-8}, 8.79×10^{-9}, 3.65×10^{-9} and 2.43×10^{-8} M·S^{-1}, respectively. The K_{cat} OPD of $Na_8H[\alpha\text{-}PW_9O_{34}]$, $Na_{10}[\alpha\text{-}SiW_9O_{34}]$, $Na_{10}[\alpha\text{-}GeW_9O_{34}]$ and $Na_{10}H_2W_{12}O_{42}$ were $4.912 \times 10^{-4}\,S^{-1}$, $2.02 \times 10^{-4}\,S^{-1}$, $7.03 \times 10^{-4}\,S^{-1}$ and $1.46 \times 10^{-4}\,S^{-1}$. The values for K_m H_2O_2 of $Na_8H[\alpha\text{-}PW_9O_{34}]$, $Na_{10}[\alpha\text{-}SiW_9O_{34}]$, $Na_{10}[\alpha\text{-}GeW_9O_{34}]$ and $Na_{10}H_2W_{12}O_{42}$ were 13.81, 63.55, 44.05, and 132.03 mM, respectively. The V_{max} H_2O_2 of $Na_8H[\alpha\text{-}PW_9O_{34}]$, $Na_{10}[\alpha\text{-}SiW_9O_{34}]$, $Na_{10}[\alpha\text{-}GeW_9O_{34}]$ and $Na_{10}H_2W_{12}O_{42}$ were 8.19×10^{-9}, 6.07×10^{-8}, 1.69×10^{-8} and 3.22×10^{-7} M·S^{-1}, respectively. The values for K_{cat} H_2O_2 of $Na_8H[\alpha\text{-}PW_9O_{34}]$, $Na_{10}[\alpha\text{-}SiW_9O_{34}]$, $Na_{10}[\alpha\text{-}GeW_9O_{34}]$ and $Na_{10}H_2W_{12}O_{42}$ were $9.73 \times 10^{-6}\,S^{-1}$, $2.48 \times 10^{-5}\,S^{-1}$, $1.58 \times 10^{-4}\,S^{-1}$ and $4.26 \times 10^{-5}\,S^{-1}$, respectively. The comparison of K_m and V_{max} of peroxidase-like enzymes were listed in Table 1. It was found that $K_{10}P_2W_{18}Fe_4(H_2O)_2O_{68}$ had lower K_m than other POMs-based peroxidases with OPD or H_2O_2 as

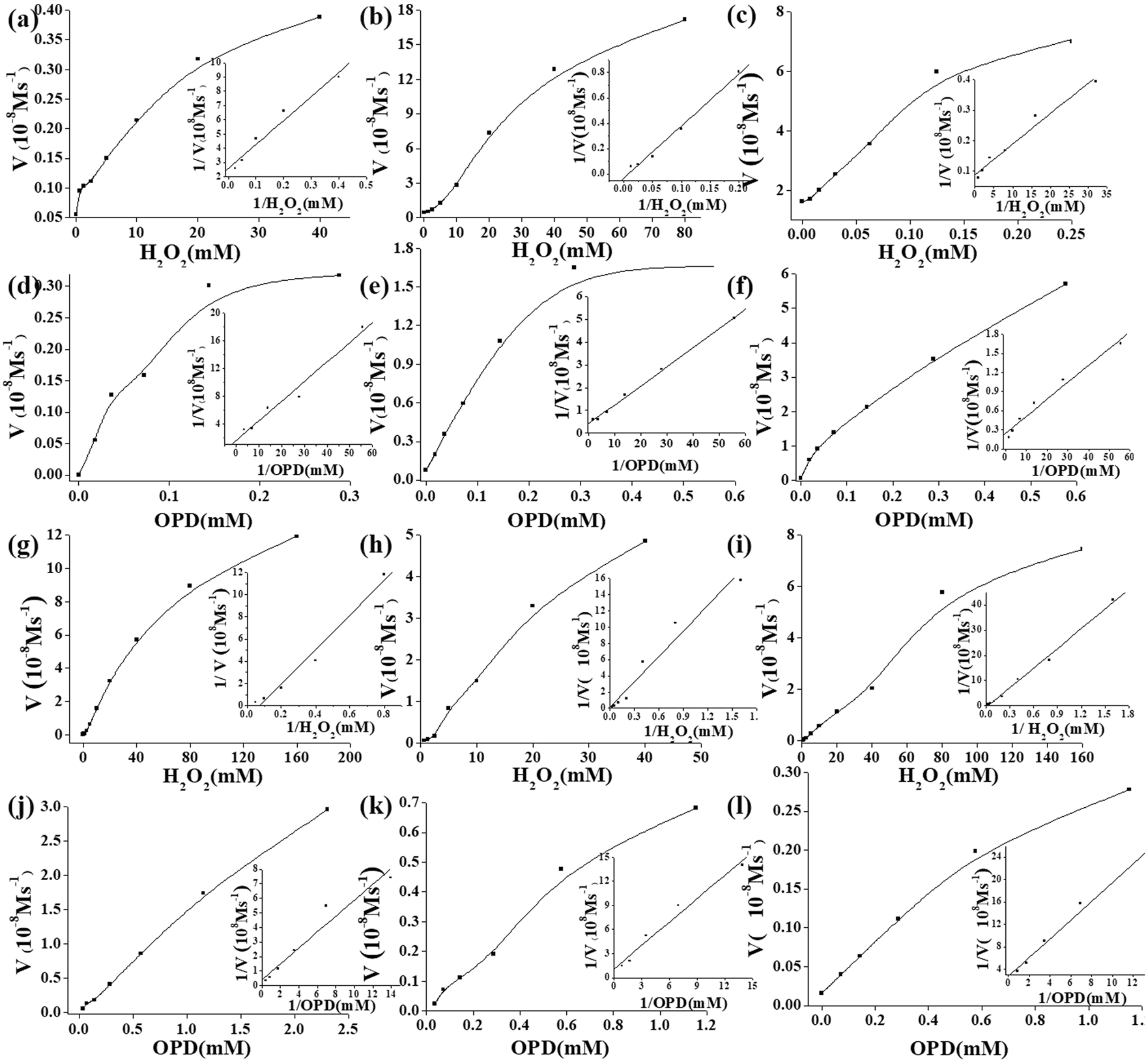

Figure 7. The steady-state kinetic assay and catalytic mechanism of peroxidase-like enzymes. (**a**,**b**) $K_{10}P_2W_{18}Fe_4(H_2O)_2O_{68}$, (**c**,**d**) $H_3PW_{12}O_{40}$, (**a**,**e**) $Na_8H[\alpha\text{-}PW_9O_{34}]$, (**b**,**f**) $Na_{10}[\alpha\text{-}SiW_9O_{34}]$, (**c**,**g**) $Na_{10}[\alpha\text{-}GeW_9O_{34}]$ and (**d**,**h**) $Na_{10}H_2W_{12}O_{42}$.

substrates. It suggests that $K_{10}P_2W_{18}Fe_4(H_2O)_2O_{68}$ might have a similar affinity for the surfaces of OPD with HRP. The mechanism of steady-state kinetics of $K_{10}P_2W_{18}Fe_4(H_2O)_2O_{68}$ were also investigated with TMB as substrates, as shown in Supplementary Fig. S8. The values for K_m and V_{max} TMB was 0.25 mM and 2.42×10^{-7} M·S^{-1}, respectively. The values for K_m and V_{max} H_2O_2 was 1.09 mM and 1.02×10^{-7} M·S^{-1}. It suggests that $K_{10}P_2W_{18}Fe_4(H_2O)_2O_{68}$ might have a similar affinity for the surfaces of TMB with HRP. The K_{cat} of $K_{10}P_2W_{18}Fe_4(H_2O)_2O_{68}$ with H_2O_2 and TMB are 4.54×10^{-2} S^{-1} and 8.82×10^{-3} S^{-1}. Comparing with the other organic-inorganic POM-based hybrids as shown in Table S1, the $K_{10}P_2W_{18}Fe_4(H_2O)_2O_{68}$ also show strong peroxidase activities with TMB as a substrate. It can be selected to construct new materials with organic groups or different nanomaterials.

The K_m and V_{max} were obtained for oxidase-like enzymes, as shown in Fig. 8. With OPD as substrates, the values of K_m OPD were 0.014, 0.013, 0.038, 0.015 and 0.015 mM for $H_3PMo_{12}O_{40}$, $H_4SiMo_{12}O_{40}$, $Eu_3PMo_{12}O_{40}$, $H_5PMo_{10}V_2O_{40}$ and α-1,2,3, $-K_6H[SiW_9V_3O_{34}]$. The V_{max} OPD of $H_3PMo_{12}O_{40}$, $H_4SiMo_{12}O_{40}$, $Eu_3PMo_{12}O_{40}$, $H_5PMo_{10}V_2O_{40}$ and α-1,2,3, -$K_6H[SiW_9V_3O_{34}]$ were 1.08×10^{-9}, 6.19×10^{-9}, 2.83×10^{-9}, 2.64×10^{-9} and 1.30×10^{-8} M·S^{-1}, respectively. The K_{cat} OPD of $H_3PMo_{12}O_{40}$, $H_4SiMo_{12}O_{40}$, $Eu_3PMo_{12}O_{40}$, $H_5PMo_{10}V_2O_{40}$ and α-1,2,3-$K_6H[SiW_9V_3O_{34}]$ were 4.32×10^{-5}, 3.09×10^{-4}, 5.66×10^{-5}, 1.32×10^{-4} and 1.73×10^{-3}S^{-1}, respectively. The comparison of K_m and V_{max} with different substrates were shown in Table 2. The value results of K_m OPD suggested that OPD have similar affinity for the surface of the oxidase-like POMs except the $Eu_3PMo_{12}O_{40}$. α-1,2,3-$K_6H[SiW_9V_3O_{34}]$ has the fastest catalytic rate than the other POMs. Among the saturated Keggin-type POMs, the counter ion Eu^{3+} maybe inhibit the poly anions interactions with the organic component. The K_m and V_{max} were also obtained with TMB as substrate, as shown in Supplementary Fig. S9. The K_m of oxidase-like enzymes was dramatically lower than natural enzyme HRP With TMB as substrates, the K_m were 0.616, 0.49, 0.086,

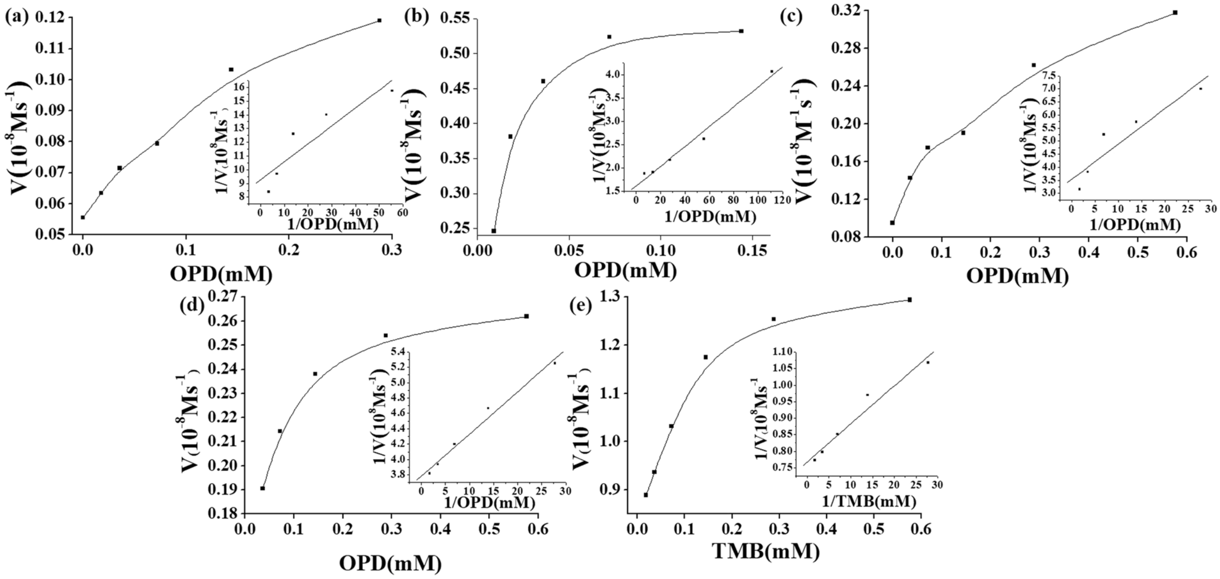

Figure 8. The steady-state kinetic assay and catalytic mechanism of oxidase-like enzymes. (**a**)$H_3PMo_{12}O_{40}$, (**b**) $H_4SiMo_{12}O_{40}$, (**c**) $Eu_3PMo_{12}O_{40}$, (**d**) $H_5PMo_{10}V_2O_{40}$, (**e**) α-1,2,3-$K_6H[SiW_9V_3O_{34}]$, (**f**) $H_6P_2Mo_{18}O_{62}$.

Nanozymes	Substrate	K_m (mM)	V_{max} (M·S^{-1})
$Na_8H[\alpha\text{-}PW_9O_{34}]$	OPD	1.39	6.14×10^{-9}
$Na_8H[\alpha\text{-}PW_9O_{34}]$	H_2O_2	13.81	3.89×10^{-9}
$Na_{10}[\alpha\text{-}SiW_9O_{34}]$	OPD	0.85	2.53×10^{-8}
$Na_{10}[\alpha\text{-}SiW_9O_{34}]$	H_2O_2	63.55	8.19×10^{-9}
$Na_{10}[\alpha\text{-}GeW_9O_{34}]$	OPD	0.61	8.79×10^{-9}
$Na_{10}[\alpha\text{-}GeW_9O_{34}]$	H_2O_2	44.05	6.07×10^{-8}
$Na_{10}H_2W_{12}O_{42}$	OPD	0.2	3.65×10^{-9}
$Na_{10}H_2W_{12}O_{42}$	H_2O_2	132.03	1.69×10^{-8}
$K_{10}P_2W_{18}Fe_4(H_2O)_2O_{68}$	OPD	0.10	2.43×10^{-8}
$K_{10}P_2W_{18}Fe_4(H_2O)_2O_{68}$	H_2O_2	0.11	3.22×10^{-7}
$H_3PW_{12}O_{40}$	OPD	0.17	4.11×10^{-8}
$H_3PW_{12}O_{40}$	H_2O_2	6.62	1.13×10^{-9}
HRP	OPD	0.59	4.65×10^{-8} [46]
HRP	H_2O_2	0.34	9.48×10^{-8} [46]

Table 1. Comparison of the K_m and V_{max} of peroxidase-like enzymes.

Nanozymes	Substrate	K_m (mM)	V_{max} (M·S^{-1})	Reference
$H_3PMo_{12}O_{40}$	OPD	0.014	1.08×10^{-9}	This work
$H_3PMo_{12}O_{40}$	TMB	0.625	2.25×10^{-7}	This work
$H_4SiMo_{12}O_{40}$	OPD	0.013	6.19×10^{-9}	This work
$H_4SiMo_{12}O_{40}$	TMB	0.522	2.25×10^{-7}	This work
$Eu_3PMo_{12}O_{40}$	OPD	0.038	2.83×10^{-9}	This work
$Eu_3PMo_{12}O_{40}$	TMB	0.086	2.60×10^{-8}	This work
$H_5PMo_{10}V_2O_{40}$	OPD	0.015	2.64×10^{-9}	This work
$H_5PMo_{10}V_2O_{40}$	TMB	0.553	2.30×10^{-7}	This work
$H_6P_2Mo_{18}O_{62}$	TMB	0.750	5.30×10^{-7}	This work
α-1,2,3-$K_6H[SiW_9V_3O_{34}]$	OPD	0.015	1.30×10^{-8}	This work
α-1,2,3-$K_6H[SiW_9V_3O_{34}]$	TMB	0.020	1.49×10^{-8}	This work
PMV-FA	TMB	0.00041	4.70×10^{-6}	[20]
$FAPMoV_1$	TMB	2.6×10^{-3}	1.33×10^{-6}	[47]
$FAPMoV_3$	TMB	0.32×10^{-3}	1.46×10^{-5}	[47]

Table 2. Comparison of the K_m and V_{max} of oxidase-like enzymes.

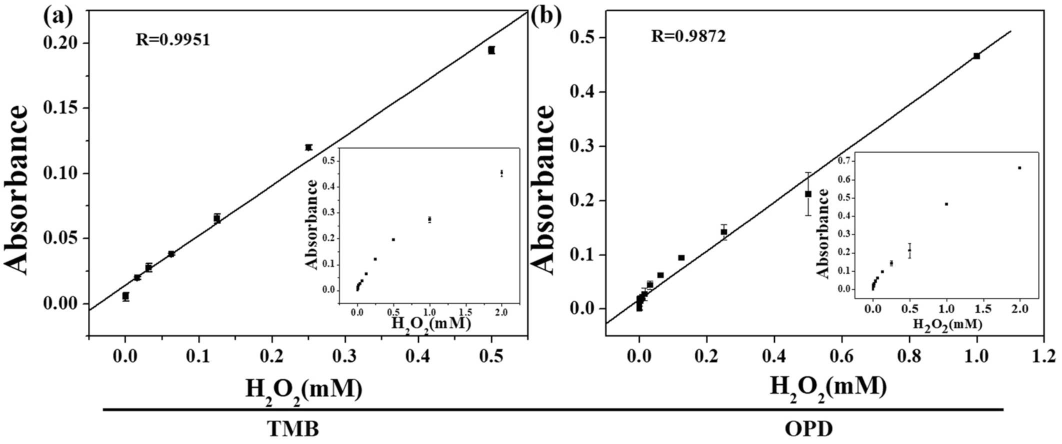

Figure 9. A does-response curve for $K_{10}P_2W_{18}Fe_4(H_2O)_2O_{68}$ depending of the absorbance at 450 nm with OPD as substrates and at 650 nm with TMB as substrates in the presence of diverse concentrations of H_2O_2. (**a**)TMB as substrates; (**b**) OPD as substrates.

0.55, 0.02, 0.75 mM for $H_3PMo_{12}O_{40}$, $H_4SiMo_{12}O_{40}$, $Eu_3PMo_{12}O_{40}$, $H_5PMo_{10}V_2O_{40}$, α-1,2,3-$K_6H[SiW_9V_3O_{34}]$ and $H_6P_2Mo_{18}O_{62}$. The V_{max} of $H_3PMo_{12}O_{40}$, $H_4SiMo_{12}O_{40}$, $Eu_3PMo_{12}O_{40}$, $H_5PMo_{10}V_2O_{40}$, α-1,2,3-$K_6H[SiW_9V_3O_{34}]$ and $H_6P_2Mo_{18}O_{62}$ were 2.25×10^{-7}, 2.25×10^{-7}, 2.60×10^{-8}, 2.30×10^{-7}, 1.49×10^{-8}, 5.30×10^{-7} $M{\cdot}S^{-1}$, respectively. The K_{cat} of $H_3PMo_{12}O_{40}$, $H_4SiMo_{12}O_{40}$, $Eu_3PMo_{12}O_{40}$, $H_5PMo_{10}V_2O_{40}$, α-1,2,3-$K_6H[SiW_9V_3O_{34}]$ and $H_6P_2Mo_{18}O_{62}$ were 9.00×10^{-3}, 1.13×10^{-2}, 5.20×10^{-4}, 1.15×10^{-2}, 1.98×10^{-3} and $2.12 \times 10^{-7}S^{-1}$, respectively.

Detection of the reactive hydroxyl radicals ·OH production. The mechanism of peroxidase-like activity of POMs originates from their catalytic ability to the decomposition of H_2O_2 to produce hydroxyl radical (·OH). Terephthalic acid (TA) can capture ·OH to generate 2-hydroxy terephthalic acid (HTA) which can be detected by fluorescence method. So we chose TA as fluorescence probe to detect the generation of ·OH. As show in Supplementary Fig. S10, the control groups (TA, TA with H_2O_2 and TA with POMs) did not show the significant intensity for HTA. Only in the presence of POMs and H_2O_2, the fluorescence can be remarkable found. This supported that the POMs can catalyze the H_2O_2 to generate ·OH, then justify the peroxidase-like activities of POMs.

Calibration curve for H_2O_2 detection. Because the $K_{10}P_2W_{18}Fe_4(H_2O)_2O_{68}$ has the strongest the peroxidase mimetic activity, it can be used in the sensing for H_2O_2. Under optimum conditions, a colorimetric assay for the detection of hydrogen peroxide based on the peroxidase-like activity of $K_{10}P_2W_{18}Fe_4(H_2O)_2O_{68}$ has been established with TMB and OPD as substrates, as shown in Fig. 9. When the substrate was TMB, the linear detection range was estimated to be from 15 to 1000 μM with correlation coefficients 0.9951. The lower limit of detection (LOD) of $K_{10}P_2W_{18}Fe_4(H_2O)_2O_{68}$ was 10.43 μM. When the substrate was OPD, the correlation between the absorption value and H_2O_2 concentration were linear over the range of 15–500 μM with correlation coefficients 0.9872. The lower limit of detection (LOD) of $K_{10}P_2W_{18}Fe_4(H_2O)_2O_{68}$ was 8.86 μM. In addition, the analytical performance of $K_{10}P_2W_{18}Fe_4(H_2O)_2O_{68}$ as peroxidase mimics was compared with others reported POM, HRP and nanozymes, as summarized in Table 3. By comparing with other enzyme mimics, it revealed that the $K_{10}P_2W_{18}Fe_4(H_2O)_2O_{68}$ sensor has wider linear range.

Conclusion

In conclusion, the structures, the hybrid atoms, the coordination atoms, the substituted metal atoms are the effect factors for their enzyme mimic activities. The polyoxomolybdates ($H_3PMo_{12}O_{40}$, $H_4SiMo_{12}O_{40}$ and $Eu_3PMo_{12}O_{40}$) have shown oxidase-like enzymes activities, while the polyoxotungstates shows peroxidase mimic activities. The substituted metals improved the enzyme mimic activities of POMs, which proved in $H_5PMo_{10}V_2O_{40}$, α-1,2,3-$K_6H[SiW_9V_3O_{34}]$ and $K_{10}P_2W_{18}Fe_4(H_2O)_2O_{68}$. The affinity of POM with substrate is another important factor on their enzyme mimic activities. For example, the $Na_{10}H_2W_{12}O_{42}$, $Na_8H[\alpha\text{-}PW_9O_{34}]$, $Na_{10}[\alpha\text{-}SiW_9O_{34}]$ and $Na_{10}[\alpha\text{-}GeW_9O_{34}]$ possessed peroxidase-like activities only with OPD as the substrates. pH condition is the key impact factor not only in the stability of POM but also the enzymes activities of them. The lacunary-Keggin type POMs, $Na_{10}[\alpha\text{-}GeW_9O_{34}]$, $Na_8H[\alpha\text{-}PW_9O_{34}]$ and $Na_{10}[\alpha\text{-}SiW_9O_{34}]$ were firstly found to own strong catalytic activities under alkaline conditions. Interesting, $K_{10}P_2W_{18}Fe_4(H_2O)_2O_{68}$ showed the highest catalytic activities among the POMs. In the future, the further analysis the inorganic systems and functionalization of metal-substituted polyoxotungstates will be expected to have a potential application in biotechnology, clinical diagnosis and other industry to substitute natural enzymes.

Experimental

Chemicals and materials.

All the chemicals used were of analysis and graded without further purification. OPD was purchased from Tianjin Guangfu Fine Chemical Research Institute (Tianjin, China). TMB was obtained from (Tokyo, Japan). $H_3PW_{12}O_{40}$, $H_4SiW_{12}O_{40}$ and $H_3PMo_{12}O_{40}$ and Hydrogen peroxide (H_2O_2, 30%) were purchased from Beijing Chemical Works (Beijing, China). The water used in the experiments was purified.

Nanozymes	Linear Range	Limit of Detection	Time	Reference
$K_{10}P_2W_{18}Fe_4(H_2O)_2O_{68}$	15–1000 μM	10.43 μM	5 min	This work[a]
$K_{10}P_2W_{18}Fe_4(H_2O)_2O_{68}$	15–500 μM	8.86 μM	5 min	This work[b]
$Cu_6(Trz)_{10}(H_2O)_4[H_2SiW_{12}O_{40}]$	10–60 μM	1.37 μM	1 min	[32]
$Na_4H_2[Cu_4(im)_{14}][Cu_3(H_2O)_3(BiW_9O_{33})_2]$	1–50 μM	0.12 μM	2 min	[28]
$Na_4H_2[Cu_4(im)_{14}][Cu_3(H_2O)_3(SbW_9O_{33})_2]$	1–50 μM	0.12 μM	2 min	[28]
FA-Fe_2SiW_{10}	0.13–67 μM	0.13 μM	1 min	[22]
FF@PW_{12}	1–75 μM	0.11 μM	10 min	[27]
$Na_4(NH_4)_{14}[Zr_4O_6(OAc)_2(P_2W_{16}O_{59})_2]\cdot 51H_2O$	100–1000 μM	100 μM	90 min	[23]
$H_4SiW_{12}O_{40}$	1–20 μM	0.4 μM	5 min	[19]
$H_3PW_{12}O_{40}$	0.1–67 μM	0.13 μM	10 min	[21]
HRP	1–60 μM	1 μM	—	[48]
Fe_3O_4 MNPs	1–100 μM	0.5 μM	—	[49]

Table 3. Comparison of different nanozymes for the detection of H_2O_2. [a]TMB as the substrate; [b]OPD as the substrate.

The POMs mimetic enzymes were characterized by IR and UV-vis spectrum. The UV-*vis* spectrum was recorded in the range of 200–600 nm on UV-Vis spectrophotometer (Puxi Inc., Beijing, China). Fourier-transform infrared spectrum (FT-IR) was collected in the range of 4000–400 cm^{-1} on an Alpha Centauri FT/IR spectrophotometer (Shizumi, Tokyo) using KBr pellets.

Synthesis of polyoxometalates. The 18 polyoxometalates including Keggin ($H_3PW_{12}O_{40}$, $H_4SiW_{12}O_{40}$, $H_4GeW_{12}O_{40}$, $K_4GeW_{12}O_{40}$, $H_4SiMo_{12}O_{40}$, $H_3PMo_{12}O_{40}$, $Eu_3PMo_{12}O_{40}$), Dawson ($H_6P_2Mo_{18}O_{62}$, α-$(NH_4)_6P_2W_{18}O_{62}$, α-$K_6P_2W_{18}O_{62}\cdot 14H_2O$), lacunary-Keggin ($Na_{10}[\alpha\text{-}GeW_9O_{34}]$, $Na_8H[\alpha\text{-}PW_9O_{34}]$, $Na_{10}[\alpha\text{-}SiW_9O_{34}]$, $K_8[\gamma\text{-}SiW_{10}O_{36}]$) and the transition-metal substituted-type (α-1,2,3-$K_6H[SiW_9V_3O_{34}]$, $H_5PMo_{10}V_2O_{40}$, Wells-Dawson ($K_{10}P_2W_{18}Fe_4(H_2O)_2O_{68}$) investigated in this study were synthesized according to the literature[36–43] or provide by prof. Yangguang Li.

Enzyme mimetic activities of POMs. The enzyme mimetic activities of POMs were determined spectrophotometrically by measuring the formation of DAB from OPD at 450 nm ($\varepsilon = 2.1 \times 10^4\ mM^{-1}\ cm^{-1}$)[44] or TMB^+ from TMB at 650 nm ($\varepsilon = 3.9 \times 10^4\ mM^{-1}\ cm^{-1}$)[45] using UV-vis spectrophotometer in a 1 cm cuvette. Typically, the 480 μL of TMB (1.5 mM in ethanol) or OPD solution (3.6 mM in water) was added into 2400 μL different buffer solutions (NaH_2PO_4-citrate or Tris-HCl), followed by the addition of 60 μL of POMs (10 mM) and 60 μL of hydrogen peroxide (H_2O_2, 10 M). The mixed solution was incubated at room temperature. The oxidases activities of POMs (10 mM) were used under the same identical reaction conditions with the absence of H_2O_2.

pH measurements. The activities of the POMs at different pH values were performed using the same condition as above, except two different buffer compositions for the different pH ranges were employed. The reaction was carried out 200 µM POMs to which TMB (240 µM) or OPD (576 μM) and H_2O_2 (200 mM) were added. Between pH 2.5 to 7, 0.2 mM of Na_2HPO_4-citrate buffer was used; for pH 7–10, 0.1 mM of Tris-HCl buffer was used. The pH of the different buffers was adjusted using a pH meter (PHS-25 pH meter, Shanghai INESA Scientific Instrument Co., China).

Determination of kinetic parameters. The steady-state kinetics of POM-peroxidase were conducted by varying the concentrations of H_2O_2 (0–200 mM), or OPD/TMB (0–576 μM/0–240 μM) one at a time. The reaction was carried out in 0.2 mM Na_2HPO_4-citrate buffer and 0.1 mM Tris-HCl (at the optimum pH) and monitored spectrophotometrically by 300 s using a 1 cm cuvette. The kinetic curves were adjusted to the Michaelis-Menten model and linear weaver-Burk linearizations were performed using origin 7.0 software. The apparent kinetic parameters were calculated based on the equation $v = V_{max} \times [S]/(K_m + [S])$, where v is the initial velocity, V_{max} is the maximal reaction velocity, [S] is the concentration of substrate, and K_m is the Michaelis constant.

Detection of the reactive hydroxyl radicals ·OH production. The hydroxyl radicals (·OH) production was measured by fluorescence method. The terephthalic acid was used as a fluorescence probe for detection the ·OH from the H_2O_2 for $Na_{10}[\alpha\text{-}GeW_9O_{34}]$, $Na_8H[\alpha\text{-}PW_9O_{34}]$, $Na_{10}[\alpha\text{-}SiW_9O_{34}]$ and $K_{10}P_2W_{18}Fe_4(H_2O)_2O_{68}$ as catalysts. 75 μL of 25 mM TA in NaOH (pH = 13) solution was added into the 3 mL of PBS (pH = 7.4) containing 100 mM H_2O_2 and/or 1 mM POMs. After 24 h incubation in the dark, the resulting solution was detected. The fluorescence spectra were obtained with excitation wavelength of 315 nm and the emission spectra were recorded in the wavelength of 425 nm.

Detection of H_2O_2. The detection of H_2O_2 was performed according to the following steps: 480 μL of OPD solution (576 μM) or TMB solution (240 μM), 60 μL of POMs (100 μM) and 60 μL H_2O_2 (200 mM) with various concentrations were added into 2400 μL of buffer solution, and the total volume of the mixed solution was 3 mL. After reacting 5 min under the optimum conditions, then the UV-Vis spectrophotometer was used to record the absorbance at 450 nm for OPD and 650 nm for TMB.

Received: 4 April 2019; Accepted: 12 September 2019;

References

1. Mozhaev, V. V., Sergeeva, M. V., Belova, A. B. & Khmelnitsky, Y. L. Multipoint attachment to a support protects enzyme from inactivation by organic solvents: α-chymotrypsin in aqueous solutions of alcohols and diols. *Biotechnol. Bioeng.* **35**, 653–659 (1990).
2. Burton, S. G., Cowan, D. A. & Woodley, J. M. The search for the ideal biocatalyst. *Nat. Biotechnol.* **20**, 37–45 (2002).
3. Rreslow, R. & Overman, L. E. "Artificial enzyme" combining a metal catalytic group and a hydrophobic binding cavity. *J. Am. Chem. Soc.* **92**, 1075–1077 (1970).
4. R. Breslow, Artificial enzymes, *Wiley-VCH*, Weinheim. (2005).
5. Raynal, M., Ballester, P., Vidal-Ferran, A. & Van Leeuwen, P. W. N. M. Supramolecular catalysis. Part 1: non-covalent interactions as a tool for building and modifying homogeneous catalysts. *Chem. Soc. Rev.* **43**, 1734–1787 (2014).
6. Aiba, Y., Sumaoka, J. & Komiyama, M. Artificial DNA cutters for DNA manipulation and genome engineering. *Chem. Soc. Rev.* **40**, 5657–5668 (2011).
7. Gao, L. Z. *et al.* Intrinsic peroxidase-like activity of ferromagnetic nanoparticles. *Nat. Nanotechnol.* **2**, 577–583 (2007).
8. Wei, H. & Wang, E. K. Nanomaterials with enzyme-like characteristics (nanozymes): next-generation artificial enzymes. *Chem. Soc. Rev.* **42**, 6060–6093 (2013).
9. Wei, H. & Wang, E. K. Fe_3O_4 magnetic nanoparticles as peroxidase mimetics and their applications in H_2O_2 and glucose detection. *Anal. Chem.* **80**, 2250–2254 (2008).
10. Kuah, E., Toh, S., Yee, J., Ma, Q. & Gao, Z. Q. Enzyme mimics: advances and applications. *Chem. Eur. J.* **22**, 8404–8430 (2016).
11. Komkova, M. A., Karyakina, E. E. & Karyakin, A. A. Catalytically synthesized prussian blue nanoparticles defeating natural enzyme peroxidase. *J. Am. Chem. Soc.* **140**, 11302–11307 (2018).
12. Long, D. L., Tsunashima, R. & Cronin, L. Polyoxometalates: building blocks for functional nanoscale systems. *Angew. Chem. Int. Edit* **49**, 1736–1758 (2010).
13. Pope, M. T. & Müller, A. Polyoxometalate chemistry: an old field with new dimensions in several disciplines. *Angew. Chem. Int. Edit.* **30**, 34–48 (1991).
14. Ma, Y. Y. *et al.* Highly efficient hydrogen evolution from seawater by a low-cost and stable CoMoP@C electrocatalyst superior to Pt/C. *Energ. Environ. Sci.* **10**, 788–798 (2017).
15. Li, J. S. *et al.* Coupled molybdenum carbide and reduced graphene oxide electrocatalysts for efficient hydrogen evolution. *Nat. Commun.* **7**, 11204 (2016).
16. Wang, S. S. & Guo, Y. Y. Recent advance in polyoxometalate-catalyzed reactions. *Chem. Rev.* **115**, 4893–4962 (2015).
17. Long, D. L., Tsunashima, R. & Cronin, L. Polyoxometalates: building blocks for functional nanoscale systems. *Angew. Chem.* **122**, 1780–1803 (2010).
18. Mizuno, N., Yamaguchi, K. & Kamata, K. Epoxidation of olefins with hydrogen peroxide catalyzed by polyoxometalates. *Coord. Chem. Rev.* **249**, 1944–1956 (2005).
19. Liu, S. *et al.* Fast and sensitive colorimetric detection of H_2O_2 and glucose: a strategy based on polyoxometalate clusters. *Chempluschem.* **77**, 541–544 (2012).
20. Wang, J. J., Mi, X. G., Guan, H. Y., Wang, X. H. & Wu, Y. Assembly of folate-polyoxometalate hybrid spheres for colormetric immunoassay like oxidase. *Chem. Commun.* **47**, 2940–2942 (2011).
21. Wang, J. J., Han, D. X., Wang, X. H., Qi, B. & Zhao, M. S. Polyoxometalates as peroxidase mimetics and their applications in H_2O_2 and glucose detection. *Biosens. Bioelectron.* **36**, 18–21 (2012).
22. Sun, Z. *et al.* Fabrication of inorganic-organic hybrid based on polyoxometalates $SiW_{10}Fe_2$ and folate as peroxidases for colormetric immunoassay of cancer cells. *Chinese Chem. Lett.* **24**, 76–78 (2013).
23. Li, D. *et al.* Modification of tetranuclear zirconium-substituted polyoxometalates- syntheses, structures, and peroxidase-like catalytic activities. *Chem. Eur. J.* **24**, 1926–1934 (2013).
24. Duan, X. X. *et al.* Fabrication of metal-substituted polyoxometalates for colorimetric detection of dopamine and ractopamine. *Materials.* **11**, 674–684 (2018).
25. Zeb, A. *et al.* Intrinsic peroxidase-like activity and enhanced photo-Fenton reactivity of iron-substituted polyoxometalate nanostructures. *Dalton Trans.* **47**, 7344–7352 (2018).
26. She, S. *et al.* Aliphatic organoimido derivatives of polyoxometalates containing a bioactive ligand. *Chem. Eur. J.* **51**, 16987–16994 (2014).
27. Ma, Z. *et al.* Effective synergistic effect of dipeptide-polyoxometalate-graphene oxide ternary hybrid materials on peroxidase-like mimics with enhanced performance. *ACS Appl. Mater. Interfaces.* **39**, 22036–22045 (2015).
28. Chai, D. F. *et al.* Synergistic effect of sandwich polyoxometalates and copper-imidazole complexes for enhancing the peroxidase-like activity. *RSC Adv.* **5**, 78771–78779 (2015).
29. Li, X. *et al.* Keggin polyoxometalates based hybrid compounds containing helix/nanocages for colormetric biosensing. *J. Solid State Chem.* **265**, 372–380 (2018).
30. Narkhede, N., Uttam, B. & Rao, C. P. Inorganic-organic covalent hybrid of polyoxometalate-calixarene: Synthesis, characterization and enzyme activity. *Inorg. Chim. Acta.* **483**, 337–342 (2018).
31. Chen, K. *et al.* Improved peroxidase-mimic property: Sustainable, high efficiency interfacial catalysis with H_2O_2 on the surface of vesicles of hexavanadate-organic hybrid surfactants. *Nano Res.* **3**, 1313–1321 (2018).
32. Zhou, E. L. *et al.* A stable polyoxometalate-pillared metal-organic framework for proton-conducting and colormetric biosensing. *Chem. Eur. J.* **21**, 11894–11898 (2015).
33. Li, X. *et al.* Synthesis, structure and effective peroxidase-like activity of a stable polyoxometalate-pillared metal-organic framework with multinuclear cycles. *Polyhedron* **151**, 206–212 (2018).
34. Zhao, J. W. *et al.* Lanthanide-Connecting and Lone-Electron-Pair Active Trigonal-Pyramidal-AsO_3 Inducing Nanosized Poly(polyoxotungstate) Aggregates and Their Anticancer Activities. *Sci. Rep.* **6**, 26406–26418 (2016).
35. Tian, R., Zhang, B. Y., Zhao, M. M., Ma, Q. & Qi, Y. F. Polyoxometalates as promising enzyme mimics for the sensitive detection of hydrogen peroxide by fluorometric method. *Talanta.* **188**, 332–338 (2018).
36. Rocchiccioli-Deltcheff, C., Fournier, M., Franck, R. & Thouvenot, R. Chemlnform abstract: vibrational investigations of polyoxometalates.2. evidence for anion-anion interactions in molybdenun(VI) compounds related to the keggin structure. *Inorg. Chem.* **22**, 207 (1993).

37. Romanelli, G. P. *et al.* Silicagel-supported $H_6P_2W_{18}O_{62}.24H_2O$: a reusable catalyst to prepare diphenylmethyl (DPM) ethers. *ARKIVOC* **1**, 1 (2017).
38. Tézé, A., Hervé, G., Finke, R. G. & Lyon, D. K. α-, β-, and γ-Dodecatungstosilicic acids: isomers and related lacunary compounds. *Inorganic Syntheses.* **27**, 85–96 (2007).
39. Allmann, R. Die Struktur des Ammoniumparawolframates $(NH_4)_{10}[H_2W_{12}O_{42}].10H_2O$. *Acta. Cryst.* **B27**, 1393–1404 (1971).
40. Domaille, P. J. 1- and 2-dimensinal tungsten-183 and vanadium-51 NMR characterization of isopolymetalates and heteropolymetalates. *J. Am. Chem. Soc.* **106**, 7677–7687 (1984).
41. Tang, Y. & Zhang, J. Direct oxidation of benzene to phenol catalyzed by vanadium substituted heteropolymolybdic acid. *Transit. Metal Chem.* **31**, 299–305 (2006).
42. Finke, R. G., Droege, M. W. & Domaille, P. J. Trivacant heteropolytungstate derivative. 3 rational syntheses, characterization, two-dimensional ^{183}W NMR, and properties of $P_2W_{18}M_4(H_2O)_2O_{68}{}^{10-}$ and $P_4W_{30}M_4(H_2O)_2O_{112}{}^{16-}$ (M=Co, Cu, Zn). *Inorg. Chem.* **6**, 3886–3896 (1987).
43. Barats, D., Leitus, G., Biro, R. P., Shimon, L. J. W. & Neurmann, R. A stable 'end-on' iron(III)-hydroperoxo complex in water derived from a multi-iron(II)-substituted polyoxometalate and molecular oxygen. *Angew. Chem. Int. Ed.* **47**, 9908–9912 (2008).
44. Tyagi, N. & Mathur, P. Iron (III) complexes of bis (benzimidazole-2-yl) methyl thiophene-2,5-dicarboxamide: synthesis, spectral and oxidation of o-phenylenediamine. *Spectrochim. Acta. A.* **96**, 759–767 (2012).
45. Gao, Z. Q., Xu, M. D., Hou, L., Chen, G. N. & Tang, D. P. Irregular-shaped platinum nanoparticles as peroxidase mimics for highly efficient colorimetric immunoassay. *Anal. Chim. Acta.* **776**, 79–86 (2013).
46. Liu, X. *et al.* BSA-templated MnO_2 nanoparticles as both peroxidase and oxidase mimics. *Analyst.* **137**, 4552–4558 (2012).
47. Ji, Y. *et al.* Inorganic-bimolecular hybrids based on polyoxometalates: intrinsic oxidase catalytic activity and their application to cancer immunoassay. *Sens. Actuators B.* **208**, 497–504 (2015).
48. Edgar, P. & Yona, K. A Simple Colorimetric Method for the measurement of hydrgen peroxide produced by cells in culture. *J. Immunol. Methods.* **38**, 161–170 (1980).
49. Kim, M. I., Shim, J., Li, T., Lee, J. & Park, H. G. Fabrication of nanoporous nanocomposites entrapping Fe_3O_4 magnetic nanoparticles and oxidases for colorimetric biosensing. *Chem. Eur. J.* **17**, 10700–10707 (2011).

Acknowledgements

This work was financially supported by NSFC (81402719) and Norman Bethune Program of Jilin University (2015228). We highly appreciate Prof. Yangguang Li from the Institute of Polyoxometalate Chemistry, Department of Chemistry, Northeast Normal University for the POMs. The open project of the CAS Key Laboratory for Biomedical Effects of Nanomaterials and Nanosafety (NKSF201801).

Author contributions

Y.Q. conceived and designed the experiment, B.Z. performed the experiments and analyzed the data. Y.Q. contributed reagents/materials/analysis tools, B.Z., M.Z., R.T., B.C., H.Z., C.Z. and C.W. wrote the paper. All authors reviewed the manuscript.

Competing interests

The authors declare no competing interests.

Additional information

Supplementary information is available for this paper at https://doi.org/10.1038/s41598-019-50539-9.

Correspondence and requests for materials should be addressed to Y.Q.

Reprints and permissions information is available at www.nature.com/reprints.

Publisher's note Springer Nature remains neutral with regard to jurisdictional claims in published maps and institutional affiliations.